Potassium channel of cardiac sarcoplasmic reticulum is a multi-ion channel

Joseph A. Hill, Jr., Roberto Coronado,* and Harold C. Strauss
Departments of Medicine and Pharmacology, Duke University Medical Center, Durham, North Carolina 27710; and
*Department of Physiology and Molecular Biophysics, Baylor College of Medicine, Houston, Texas 77030

ABSTRACT We have characterized mechanisms of ionic permeation in the K channel of canine cardiac sarcoplasmic reticulum (SR K channel). Ionic selectivity, as measured by relative permeabilities, followed Eisenman sequence I, a low field strength sequence. Slope conductance measured in symmetrical solutions across the bilayer followed Eisenman sequence V. In all cases, the selectivity characteristics of the prominent subconductance state (O_1) were similar to those of the main-state (O_2). Further, our studies have revealed that this channel differs in three significant ways from the highly characterized SR K channel of skeletal muscle. First, the ratio of permeabilities Cs^+ to K^+ was a complex function of ion concentration. Second, the concentration dependence of conductance was not well described by the Michaelis-Menten formalism. Instead, we modeled the observed relations using a more general approach based on classical rate theory. Third, mole fraction experiments (Cs^+ with K^+) demonstrated a prominent anomalous effect. Certain of our Cs^+ data required the Eyring rate theory approach for adequate interpretation. We adopted a symmetrical energy profile incorporating ion–ion interaction and thereby accounted for much of the data. We conclude that the canine cardiac SR K channel is significantly different from that of skeletal muscle, and it may accommodate more than one ion at a time.

INTRODUCTION

The electrical activity of sarcoplasmic reticulum (SR) membrane has been the subject of much scientific interest (for a review, see Caillé et al., 1985) Two broad approaches have been utilized to date, namely, measurements of transmembrane potential and studies of membrane permeability. The discovery that the SR is highly permeable to monovalent cations led to the proposal that a charge compensating mechanism existed during the Ca^{2+} fluxes associated with excitation–contraction coupling. This shunt permeability was attributed to a monovalent cation channel (McKinley and Meissner, 1978; Meissner and McKinley, 1982). In subsequent studies, this cation channel of skeletal muscle has been characterized extensively, largely through measurements of unitary channel current in artificial bilayer membranes (e.g., Miller and Racker, 1976; Coronado and Miller, 1979, 1980, 1982; Cukierman et al., 1985).

A number of studies of the skeletal muscle SR K channel have demonstrated single ion behavior, i.e., a pore that accommodates at most one ion at a time (Coronado et al., 1980; Cukierman et al., 1985). It is well known, however, that many K channels exhibit multi-ion conduction (Hille, 1984). In order to investigate this apparent discrepancy, we decided to re-examine the question of multiple-versus single-ion conduction in the SR K channel from cardiac muscle.

Confirming previous findings, we argue that permeability is modulated by a relatively weak electric field inside the pore. We describe experiments using Cs^+, a species that permeates the channel and yet impedes the diffusion of K^+, to induce a state of rapid "block." Certain experimental observations, however, are most consistent with multiple ion occupancy. Thus, our data suggest that significant differences exist between the SR K channels of mammalian cardiac and skeletal muscle. We have interpreted our findings using a two-binding site model of ionic diffusion based on classical rate theory.

Address correspondence to Harold C. Strauss, M.D., Box 3845, Room 345 Bell Building, Duke University Medical Center, Durham, NC 27710

METHODS

Experimental techniques

Bilayer phospholipid (Avanti Polar Lipids, Inc., Birmingham, AL) was suspended in *n*-decane (20–40 mg lipid/ml). Lipid suspensions were prepared as 1:1 (wt/wt) mixtures of phosphatidylethanolamine/phosphatidylserine (PE, *E. coli*:PS, bovine brain). Decane was purified by passage over a 10-cm adsorbent column of alumina (No. A-1522, Type WN-6, Neutral; Sigma Chemical Co., St. Louis, MO).

An aperture (300-μm diam) in an acrylic partition separating two chambers (3-ml *cis* and 5.5-ml *trans*) was painted with the lipid suspension (Mueller et al., 1962). Using an agar bridge electrode, the *cis* chamber was connected to a voltage-command signal. The *trans* chamber was connected to a current–voltage converter circuit (1 GΩ feedback resistor) in order to monitor transmembrane current. The signal was low-pass filtered (−3 dB generally at 100–200 Hz) using an 8-pole

0006-3495/89/01/35/12 $2.00

Bessel filter and stored on magnetic tape (Store 4-DS; Racal Recorders Inc., Sarasota, FL).

All bath electrolyte solutions were buffered with 10-mM histidine and pH adjusted to 7.1. All experiments were performed using symmetrical concentrations of solution (denoted [X] across the bilayer, unless otherwise indicated). Junction potentials were measured (and corrections assigned assuming constant charge accumulation with time) after each experiment; these were generally <3 mV in absolute value.

Vesicles were incorporated into the planar bilayer by a Ca^{2+}-induced fusion process (Miller and Racker, 1976). Fusion was halted as soon as discrete channel fluctuations were detected, usually by perfusing away the vesicle suspension. Sometimes we chose to decrease average vesicle size by sonication in a bath-type sonicator (Ultrasonic Apparatus G-112-SP1, Laboratory Supplies Co., Hicksville, NY) in order to prevent the incorporation of several channels with a fusion event (Miller and Racker, 1976).

In some experiments, it was necessary to change the solution on one side of the bilayer. To do this, we perfused the *cis* chamber with new solution while removing an identical volume of *cis* solution, all in the presence of vigorous stirring. The perfusion time required for nearly complete turnover of the bath solution was determined to be 7 min (18 ml or 6 chamber vol). Under these conditions, 0.75% (±0.20) of the original solution concentration remained (time constant = 1.42 ± 0.08 min; $n = 3$).

Data analysis

Analog single channel current data were sampled for digital analysis and stored on magnetic media. (The programs used for analysis were kindly provided by Dr. H. Affolter, Yale University.) We routinely calculated current amplitude histograms and fitted Gaussian curves (by eye) to the approximately normally distributed current data. The amplitude of a single channel transition was taken as the difference between the means of two fitted curves. Data are reported as mean ± standard error of the mean (SEM).

Most points on all I-V curves represent the average of 3–10 amplitude calculations. A theoretical curve was fitted to the experimental I-V relation; this was generally a least squares fitted straight line. All conductances were calculated from I-V curves defined by at least three (generally 10–15) points. Reversal potentials were determined by interpolation using the fitted curve. Where noted, ratios of permeabilities were calculated using the Goldman-Hodgkin-Katz equation from reversal potential measurements taken under biionic conditions.

Vesicle preparation and characterization

Isolation procedure

Canine cardiac membrane vesicles were isolated according to the procedure described by Jones (Jones, 1988) and according to a slightly modified protocol. In the modified procedure, we interposed 0.4 M sucrose between the 0.6 and 0.25 M layers in the discontinuous density gradient. In addition, we centrifuged the gradients overnight in a swinging bucket rotor (model SW28; Beckman Instruments, Inc., Palo Alto, CA) at 25,000 rpm (113,000 g_{max}). Each procedure provided a heterogeneous population of membrane vesicles from sarcolemma and SR. This is similar to the findings reported by others (Jones and Besch, 1984; Hungerford et al., 1984).

An enriched fraction of SR vesicles from canine cardiac muscle and rabbit fast-twitch skeletal muscle was kindly provided by Dr. G. Meissner (University of North Carolina). The SR vesicles were of light density with relatively few dihydropyridine binding sites (G. Meissner, personal communication) indicating that they originated in longitudinal SR.

Eyring rate theory model

To gain additional insight into mechanisms of ionic permeation, we implemented a two-binding site Eyring rate theory model. The theory and mathematical techniques are similar to those described by others (Läuger, 1973; Hille, 1975*a*,*b*; Hille and Schwarz, 1978; Begenisich and Cahalan, 1980). The computer code was written in Turbo Pascal (Borland International, Inc.) and was modified from a FORTRAN version kindly provided by Dr. G. S. Oxford of the Department of Physiology at the University of North Carolina. Calculations were performed using an IBM PC-AT computer. Fits to the experimental data were achieved empirically.

Briefly, the permeation pathway inside the channel is represented as a linear series of free energy peaks and troughs. This corrugated energy profile corresponds to the free energy of an ion-channel system at various positions of the ion within the membrane, in the absence of (*a*) an applied electric field, and (*b*) other ions inside the channel. Ions "jump" according to a Poisson process from one site to another over an intervening energy barrier. Reaction rates for ionic diffusion are calculated as rate constants (derived from classical rate theory and including a voltage-dependent term) multiplying occupancy probabilities for each possible state. The model has two local free energy minima that can either be empty or contain an ion. Both sites may be filled simultaneously; thus, nine possible occupancy states exist. Following the pattern of Hille and Schwarz (1978), repulsive coulombic forces are assumed to drop linearly from one well to the next and are expressed as factors multiplying the rate constants. The system of differential equations is solved using a matrix technique as described by Begenisich and Cahalan (1980). Conductances are calculated as the slope of a short segment of the current–voltage curve about the *x*-axis.

RESULTS

General features

An illustrative record of the SR K channel is depicted in Fig. 1. Immediately apparent are the characteristically slow gating kinetics and the two levels of open state current, labeled O_1 and O_2. The substate O_1 was seen in all experiments; indeed, it served as one criterion for identifying the SR K channel in bilayers (other criteria included channel conductance, slow gating kinetics, and Cs^+ blockade effects). As discussed elsewhere (Hill, J. A., R. Coronado, and H. C. Strauss, manuscript in preparation), we interpret O_1 to represent a subconductance state of the "main-state" O_2. Each state (Closed, O_1, O_2) has direct access to the other two and apparently occurs at random.

Ionic selectivity

Selectivity as measured by zero-current reversal potential

We measured reversal potentials under biionic conditions, and quantified the data as relative permeabilities of species X with respect to K^+ (P_X:P_K) for open state O_2

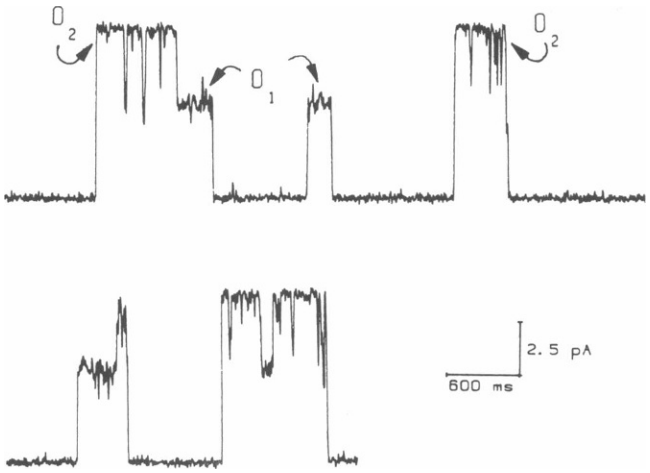

FIGURE 1 Unitary current mediated by the cardiac SR K channel with two open states (O_1, O_2).

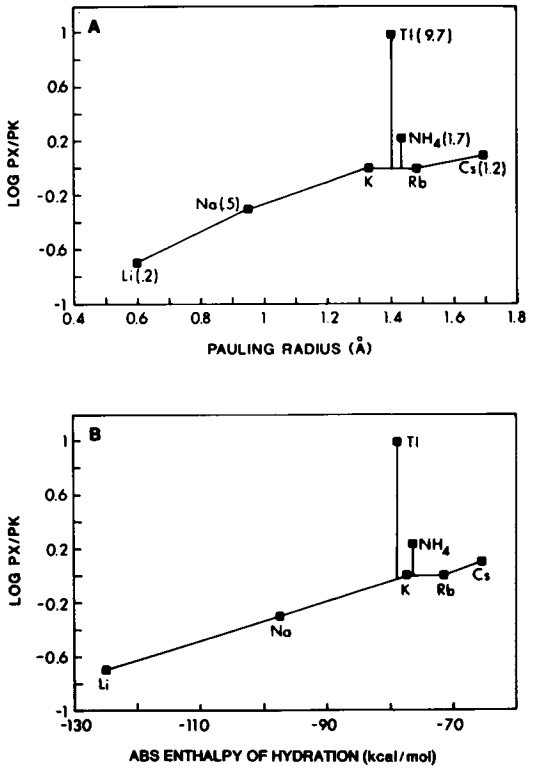

FIGURE 2 Ionic selectivity. (*A*) Selectivity fingerprint of the cardiac SR K channel. In this diagram, log permeability of species X relative to K (P_X:P_K) is plotted versus Pauling crystal radius. Reversal potentials were measured under biionic conditions, with 100 mM K^+ *trans* and 100 mM test cation X^+ *cis*. (*B*) Relative permeability is plotted as a function of absolute enthalpy of hydration.

(Fig. 2 *A*). The sequence observed, Cs (P_{Cs}:P_K = 1.25) > Rb (1) > K (1) > Na (0.5) > Li (0.2), corresponds to sequence I (low field strength) in the formalism developed by Eisenman (1961). With the notable exceptions of NH_4^+ (1.7) and Tl^+ (9.7), permeability with respect to K^+ increases monotonically with ionic radius. Other biionic potential measurements (data not shown) have confirmed that the SR K channel was Nernst ideally selective for cations over anions. Tetraethylammonium ions (TEA^+) were impermeant (P_{TEA}:P_K < 0.03) as were calcium ions (P_{Ca}:P_K unmeasurable).

The fact that permeability ratios vary directly with ionic size suggests that coulombic interactions between an alkali metal cation and water are significant in the selectivity reaction (Krasne, 1980). In other words, the permeability of a given ion is dictated largely by the ease with which surrounding water molecules are removed. A simple prediction that follows is that relative selectivity in the SR K channel should decrease with increasing hydration energy (Fig. 2 *B*). A remarkably linear relation is observed for the group IA cations.

It is apparent that NH_4^+ and Tl^+ both have anomalously high permeabilities compared with alkali metal ions of similar radius (Fig. 2 *A*) or similar hydration energy (Fig. 2 *B*). It follows (see above) that the selectivity for NH_4^+ and Tl^+ must be due at least in part to relatively greater affinities between ion and channel (as opposed to ion and water). Such effects may possibly be attributed to preferential tetrahedral associations (NH_4^+) or polarizing interactions (Tl^+) with ligands lining the channel pore (Krasne, 1980).

The selectivity fingerprint for the subconductance state O_1 was experimentally identical to that of O_2. This finding suggests that selectivity (as measured by biionic reversal potentials over the range of crystal radii 0.60 to 1.7 Å) occurs independently of the mechanism responsible for the substate. These data confirm the work of Tomlins and co-workers (Tomlins et al., 1984; Tomlins and Williams, 1986) who have shown that SR K channels from rabbit cardiac and skeletal muscle exhibit a substate with ionic selectivity characteristics similar to those of the main state.

Selectivity as measured by conductance

We measured single channel conductances in the presence of symmetrical solutions of alkali metal cations other than K^+. A representative current–voltage (I-V) curve (in Cs^+) is depicted in Fig. 3 *A* from transitions such as those shown in *B*. Current–voltage curves in Rb^+ and Na^+ also were ohmic (constructed from transitions such as those shown in *C* and *D*). Conductance data from several experiments are compiled for states O_1 and O_2 in Fig. 4. Here, selectivity as measured by conductance in the presence of symmetrical 0.1 M salt exhibited Eisenman sequence V, an intermediate field strength sequence.

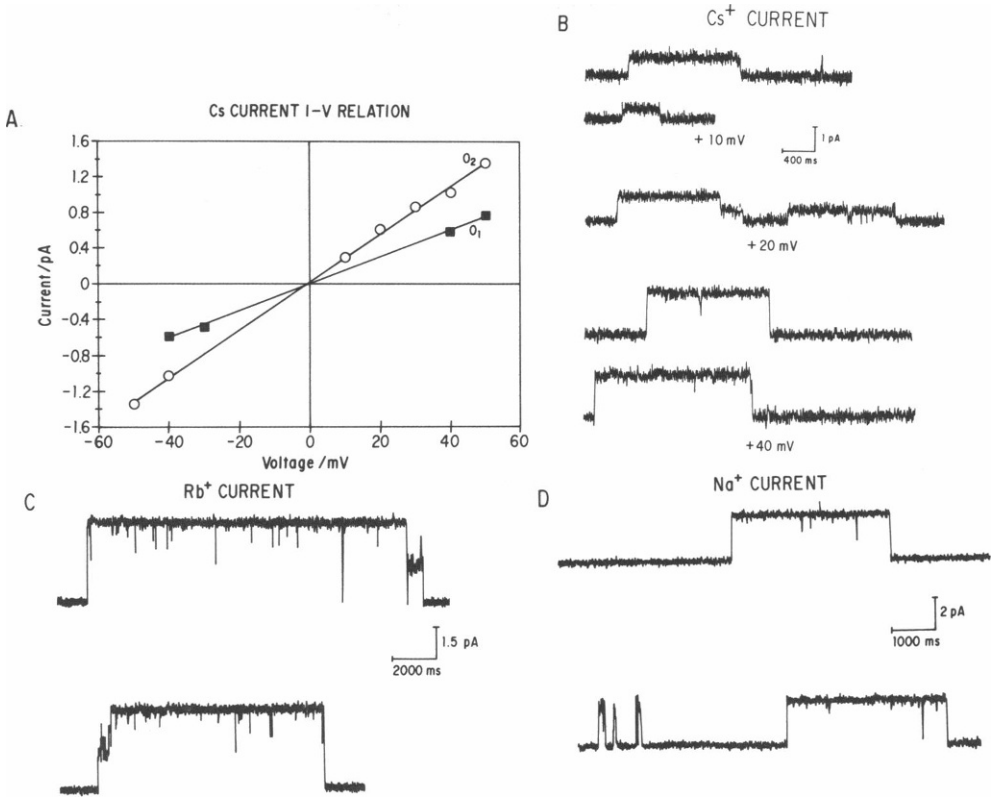

FIGURE 3 Unitary current of alkali metal cations. (*A*) Current–voltage relations recorded in symmetrical Cs^+ solutions. Experimental conditions: 327 mM CsOAc symmetrical. Slope conductances (O_2, O_1) = 35 pS, 20 pS. (*B*) Unitary current carried by Cs^+. Experimental conditions: 327 mM CsOAc // 100 mM CsOAc, V_{hold} as indicated, bandwidth = 70 Hz, open = up. Amplitudes (pA) are as follows (O_2, O_1): +40 mV, 1.8, 1.0 (not shown); +20 mV, 1.1, 0.6; +10 mV, 0.75, 0.4. Slope conductances (O_2,O_1) = 35 pS, 20 pS. (*C*) Unitary current carried by Rb^+. Experimental conditions: 327 mM RbCl // 100 mM RbCl, V_{hold} = 0 mV, bandwidth = 80 Hz, open = up. Amplitudes (pA) are 3.6 (O_2) and 1.7 (O_1). (*D*) Unitary current carried by Na^+. Experimental conditions: 280 mM NaOAc // 100 mM NaOAc, V_{hold} = +40 mV, bandwidth = 80 Hz. Amplitudes (pA) are 2.8 (O_2) and 2.1 (O_1).

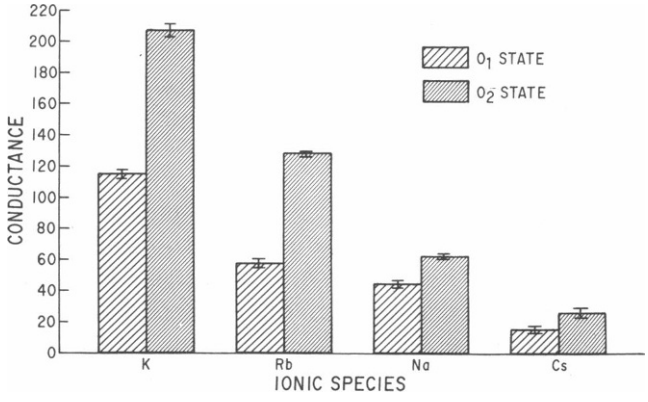

FIGURE 4 Single channel slope conductance in symmetrical 100 mM solutions. O_1 and O_2 are plotted as the mean of two or more measurements.

Again, the same selectivity sequence was observed for O_2 as for O_1.

Concentration dependence of P_{Cs}:P_K

For multi-ion channels, energy profile barrier heights as well as trough depths are important factors in ionic selectivity (Hille and Schwarz, 1978). Thus, ratios of permeabilities are expected to be functions of ionic activity and the specific energy profile of each ion. We studied the concentration dependence of P_{Cs}:P_K in two experiments. The experimental protocol involved measuring slope conductances in solutions of symmetrical concentration over the range 50–500 mM (Fig. 5). As with the selectivity fingerprint measured at 0.1 M ionic strength, the concentration dependence of P_{Cs}:P_K was identical for states O_1 and O_2. It is clear from the figure that P_{Cs}:P_K was not constant, but rather was a function of ionic activity. These results suggest that ionic permeation

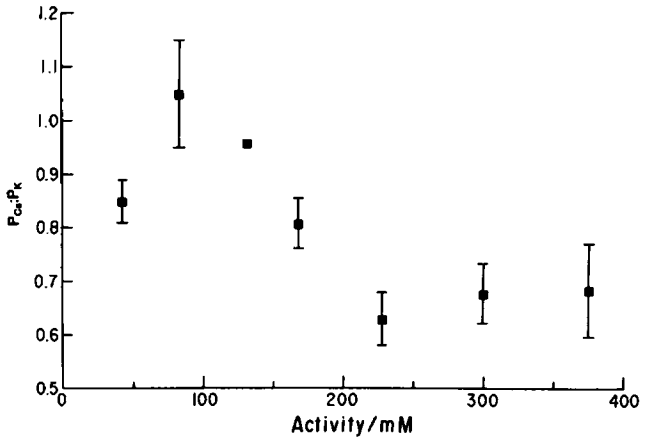

FIGURE 5 Activity dependence of relative permeability. The ratio of Cs to K permeabilities ($P_{Cs}:P_K$) is plotted versus ionic activity. Means of two or more measurements are shown ± SEM.

under these conditions involves significant ion–ion interaction.

Concentration dependence of conductance

To elucidate possible ionic interaction within the channel pore, it was necessary to know how channel conductance varied with the ionic activity of the bathing solutions. Slope conductance (O_1 and O_2) is plotted versus ionic concentration in Fig. 6 *A*. Immediately apparent is the similarity of the conductance–activity relations for O_1 and O_2. Both curves have leveled off substantially at K^+ activities of 150 mM (~200 mM concentration). An empiric fit from the permeation model (see below) is superimposed as a continuous curve on the O_2 data points. In addition, we measured the activity dependence of Na^+ conduction (Fig. 6 *B*). The ratio of conductances K^+:Na^+ (O_2) is independent of cation activity within experimental error (data not shown). Calculated data from the rate theory model (see below) are superimposed on the experimental data points in Fig. 6.

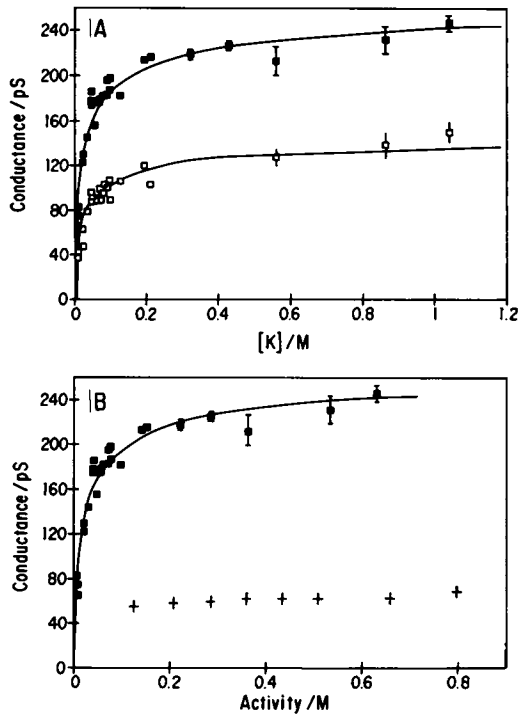

FIGURE 6 Concentration dependence of conductance. (*A*) Conductance–concentration relations for O_1 (*open squares*) and O_2 (*solid squares*) are plotted versus K concentration, [K]. Each point represents the fitted slope of a current–voltage curve (at least three points) measured in symmetrical K salt solutions. Error bars represent ± 1 unit of standard deviation. The smooth curve superimposed on O_2 is the theoretical prediction from the energy profile depicted in Fig. 10 *A*. The smooth curve superimposed on O_1 is the same as that for O_2 scaled down to 56%. (B) Slope conductances for O_2 in K^+ (*squares*) and Na^+ (*plus signs*) plotted versus ionic activity.

Cs blockade

Rapid blockade

Exposure to Cs^+ led to an apparent diminution of single channel conductance (Fig. 7). We have analyzed this effect in terms of the following simple reaction scheme:

$$Cs^+ + \text{Open} \underset{\beta}{\overset{\alpha}{\leftrightarrow}} \text{Blocked}.$$

If the forward reaction rate ($\alpha \cdot [Cs^+]$Open) and the backward rate ($\beta \cdot$ Blocked) are very rapid (with respect to the recording bandwidth), then the open state and the blocked state will be in apparent equilibrium. If the interaction between Cs^+ and the channel exceeds the bandwidth capacity of the recording apparatus, then a filtering effect blurs the two states into a single state. Under such circumstances, the two states can conveniently be considered to be a single open state, say $Open_{Cs}$. The apparent conductance of $Open_{Cs}$ is proportional to the relative dwell times of the true open and "blocked" states. For example, at low Cs^+ concentrations, the blocked state will be populated relatively infrequently, and the apparent conductance of $Open_{Cs}$ will be only slightly less than the conductance of true open state. As the Cs^+ concentration is increased, the relative importance of the blocked state will increase, and $Open_{Cs}$ current diminish. (For an alternative view of Cs^+ block

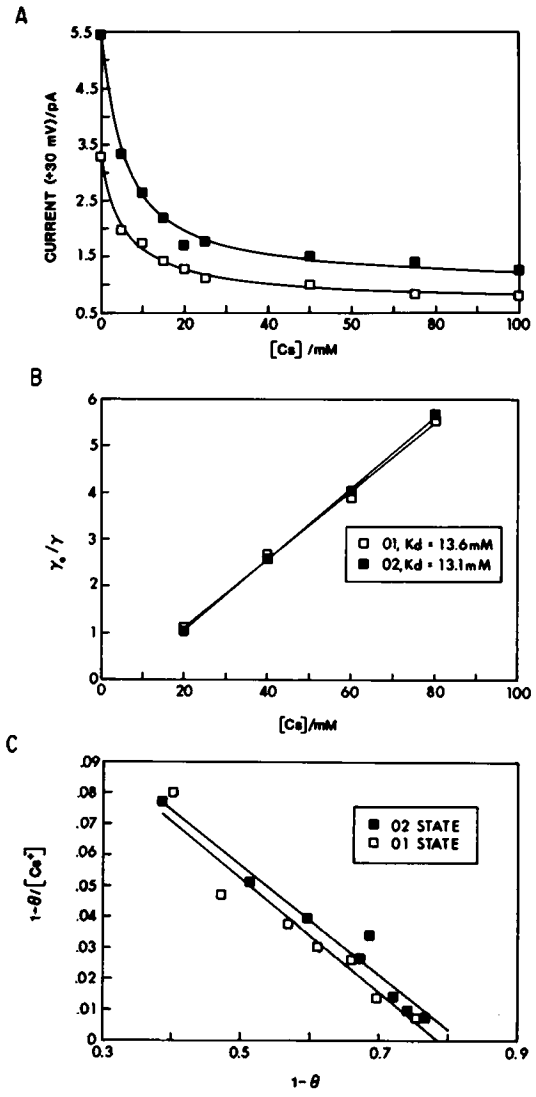

FIGURE 7 Cs blockade effects. (*A*) Conductance versus Cs concentration. Single channel current measured at +30 mV (in 100 mM K^+ from an experiment in which Cs^+ was added symmetrically across the bilayer; data are plotted versus Cs^+ concentration for O_1 (*open squares*) and O_2 (*solid squares*). The transformed relations derived from the Scatchard analysis (*C*) are superimposed. (*B*) *trans* Cs blockade. Control conductance/experimental conductance versus Cs^+ concentration (symmetrical solutions). The slopes of the fitted lines indicate that K_D (O_2, *trans*) = 13.1 mM, K_D (O_1, *trans*) = 13.6 mM. (*C*) Scatchard plots of *cis* Cs^+ blockade of the SR K channel. The fitted lines have the following parameters: O_2, K_D = 8.8 mM, sites = 0.82; O_1, K_D = 9.5 mM, sites = 0.79.

couched in terms of nonequilibrium permeation kinetics, see Discussion.)

Theoretical curves derived from the Woodhull (1973) analysis are shown superimposed on the experimental points in Fig. 7, *A* and *B*. In *C*, data from another experiment are plotted in the form of Scatchard plots. These data clearly demonstrate the similarities in binding affinity between O_1 and O_2. Collected data from six experiments (±30 mV) revealed apparent dissociation constants for the *cis* reaction: $K_D(O_1)$ = 9.5 (±1.3) mM, $K_D(O_2)$ = 8.8 (±1.0) mM, and for the *trans* reaction $K_D(O_1)$ = 16.8 (±3.2) mM, $K_D(O_2)$ = 16.0 (±3.0) mM. Measurement of Cs^+ blocking effects at relatively large transmembrane potentials consistently revealed only slight voltage-dependence of block (data not shown).

Competition of Cs block

Potassium ions compete with the blocking action of Cs^+ in the cardiac SR K channel (Fig. 8). In this figure, single channel conductance is plotted versus ionic strength from data pooled from several experiments. Each data point was recorded in 100 mM K^+ plus a variable amount of Cs^+ and/or K^+. The points that define the downward sloping curve were recorded with only Cs^+ added to the 100 mM K^+. If, however, after adding 40 mM Cs^+, K^+ activity was increased [(100 + X)mM K^+, 40 mM Cs^+] then channel conductance rose back toward control levels. This competitive behavior is additional evidence (along with the finite Cs^+ permeability) that argues strongly for a Cs^+ binding site within the pore.

Anomalous mole fraction

Finally, we investigated the mechanisms of Cs^+ interaction with K^+ transport through the SR K channel in greater detail in a mole fraction series of experiments

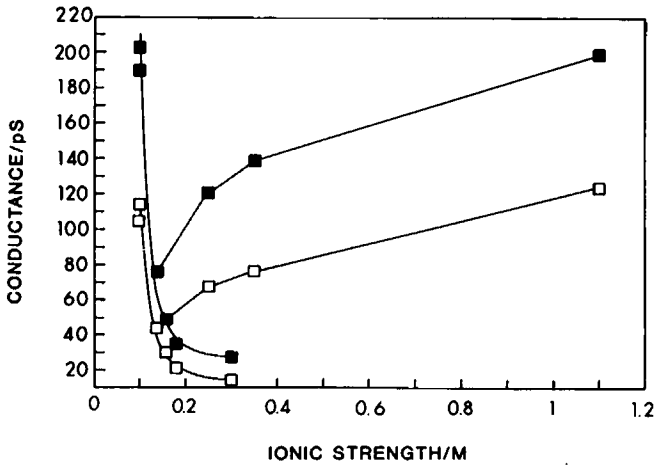

FIGURE 8 Cs^+ block is competitive with K^+. Single channel conductances (O_2, *solid squares*; O_1, *open squares*) were measured (pooled data from several experiments) initially in symmetrical 100 mM K^+. Addition of Cs^+ (up to ionic strength 0.3 M) caused a marked fall in conductance. This fall, however, is reversible by the addition of K^+ (up to ionic strength 1.1 M).

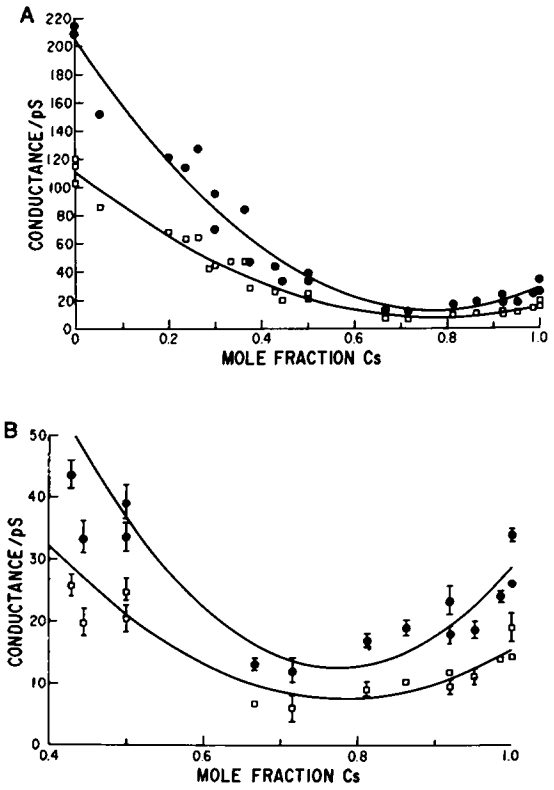

FIGURE 9 Conductance versus ionic mole fraction. (*A*) Anomalous mole fraction effect. Single channel conductance as a function of Cs^+ mole fraction (with K^+, X_{Cs}). Solutions were prepared such that $[K^+] + [Cs^+] = 200$ mM. (*B*) Close-up of anomalous mole fraction curves illustrating the conductance minimum. Error bars represent ± SEM.

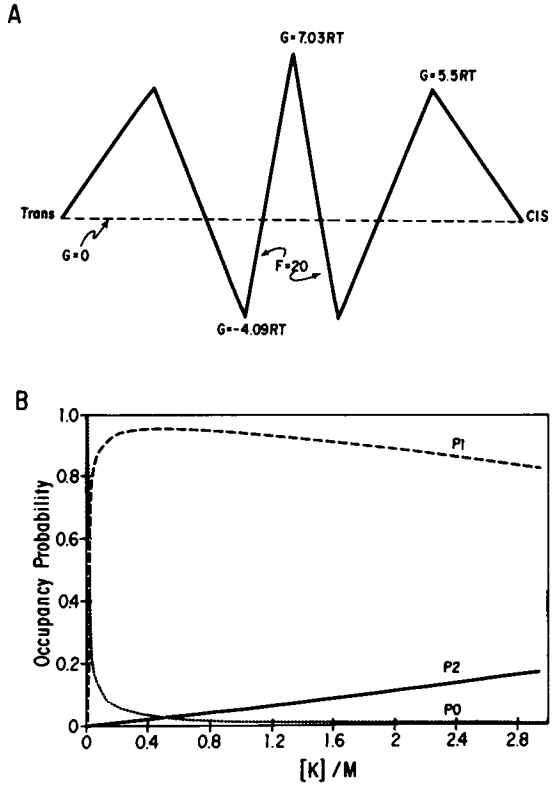

FIGURE 10 Theoretical calculations. (*A*) Free energy profile for K^+. This profile provided the best fits to current–voltage and conductance–activity data for K^+ permeation during O_2. The positions of the wells and peaks are symmetric as follows: *trans* chamber = 0.0, peak 1 = 0.2, well 1 = 0.4, peak 2 = 0.5, well 2 = 0.6, peak 3 = 0.8, *cis* chamber = 1.0. (*B*) Probabilities that a channel with an energetic profile as depicted in *A* is doubly (P_2), singly (P_1), or un- (P_0) occupied by K^+, plotted versus K^+ concentration.

(Fig. 9 *A*). In these experiments, we measured single channel conductance in the presence of symmetrical 0.2 M ionic strength ($K^+ + Cs^+$) salt solutions of varying proportions. A minimum was observed in the conductance versus Cs^+ mole fraction plot at mole fraction Cs^+ (X_{Cs}) ≈ 0.75 (Fig. 9 *B*). This minimum was identically observed for both O_1 and O_2 and strongly suggests that multiple occupancy of the channel may occur under these conditions. This property of conduction is strikingly different from that reported for the SR K channel of skeletal muscle. Fitted second degree polynomials are shown superimposed on the O_1 and O_2 data points in the illustrations; these curves are without theoretical significance.

Eyring rate theory model

We have analyzed our experimental observations in terms of a two-binding site Eyring rate theory model. Calculated data from the model are shown as continuous curves on the conductance–activity curves (Fig. 6).

The free energy profile that provided a best fit to all of the O_2 experimental data in K^+ is depicted in Fig. 10 *A*. As shown, two binding sites were necessary for an acceptable fit. As only ohmic I-V curves were observed, we adopted a symmetrical profile with lateral energy barriers of equal height (5.5 *RT*) and wells of equal depth (−4.09 *RT*). The central barrier was fixed at 7.03 *RT*. The K^+–K^+ repulsion factor was 20. Occupancy probability plots for the closed, O_1, and O_2 states are depicted in Fig. 10 *B*.

The O_1 data in K^+ were acceptably fit simply by scaling down the O_2 fit to 56% (corresponding to the ratio of their conductances) (Fig. 6). These observations are consistent with the hypothesis that the conduction pathways for K^+ during O_1 and O_2 are similar. As discussed elsewhere (Hill, J. A., R. Coronado, and H. C. Strauss, manuscript in preparation), we attribute the differences in conductance to a "duty cycle" effect for the O_1 state wherein K^+ has access to the conduction pathway only 56% of the time (flutter model).

DISCUSSION

Selectivity–relative permeability

Our measurements of ionic selectivity have confirmed findings from other SR K channels. First, the cardiac SR K channel strongly selects for cations over anions. This indicates that a negative electric field is present within the channel pore. Second, selectivity (as measured by relative permeability) is dominated by the energy required to dehydrate a cation. This implies that the electric field inside the channel pore is relatively weak (ligands are few in number, and/or have few charges or small dipole moments) and is unable to overcome the attractive forces between an ion and tightly bound water. As shown in Fig. 2 *B*, the ions from which water molecules are removed most easily are most permeant. In addition, relative permeability in the SR K channel follows in qualitative terms the mobility of alkali metal cations in aqueous solution (as measured by the diffusion coefficient, *D*): $P_X:P_K$ (*D*, 10^{-5} cm^2/s; Hille, 1984) Cs (2.06) > Rb (2.07) > K (1.96) > Na (1.33) > Li (1.03). This suggests that the permeability of a cation in the SR K channel pore is related to its mobility in aqueous solution; or an ion permeates the pore in some ways similar to the way it moves through water.

The model channels gramicidin A (Myers and Haydon, 1972) and alamethicin (Gordon, 1974) are low field strength channels. Also, the selectivity sequence described here is similar to those reported for the SR K channel of rabbit skeletal muscle (Coronado et al., 1980; Cukierman et al., 1985) namely NH_4 > K > Cs > Rb > Na > Li as well as rabbit cardiac muscle (Tomlins et al., 1984). The reported sequence for the frog SR channel is K > Na (Labarca and Miller, 1981).

Our measurements of the ratio of Cs^+ and K^+ permeabilities indicate that the ratio is a complex function of ionic activity, a result expected for a multi-ion channel (Hille and Schwarz, 1978). At present, the issue is sufficiently complicated and there are enough free variables involved that we are unable to attribute any significance to the shape of the $P_{Cs}:P_K$ relation. However, this observation is the first clue that the cardiac SR K channel exhibits significant multi-ion behavior. This observation differs from the activity-independent $P_{Cs}:P_K$ ratios reported for the SR K channel of skeletal muscle (Cukierman et al., 1985).

Conductance

Selectivity, measured as a function of conductance exhibits a different selectivity sequence, namely K > Rb > Na > Cs (Eisenman sequence V). This sequence differs substantially from that predicted from aqueous diffusion coefficients, suggesting that conduction is not simply a matter of ions moving through a water-filled pore. Again there is a large body of literature documenting biological and chemical systems that exhibit similar selectivity properties (e.g., K_m of the Na^+, K^+ ATPase of nerve, Skou, 1960; Bader and Sen, 1966; tetranactin, Krasne and Eisenman, 1976). It is interesting that the cyclic polyether XXXI, which exhibits Eisenman sequence I in certain circumstances, exhibits sequence V on salt extraction into hexane (Eisenman et al., 1968). Thus, it demonstrates the same two sequences as the canine cardiac SR K channel.

The SR K channel from frog muscle exhibits a selectivity sequence (conductance) that is quantitatively identical to that from rabbit (e.g., K > NH_4 > Rb > Na > Li > Cs). This sequence is similar to that which we describe for the canine cardiac channel (K > Rb > Na > Cs). Further, the same sequence has been observed for the rabbit cardiac SR K channel (Tomlins et al., 1984). This channel, however, exhibited similar selectivity characteristics when measured as relative permeability or conductance, a significant difference from the canine cardiac channel. Finally, the selectivity characteristics of the main conductance state and those of the substate are experimentally identical, a finding that is common to the channels from heart and skeletal muscle.

Disagreement between permeability ratios determined by conductance and zero-current potential measurements indicates that ions do not move independently. A common mechanism for violation of this "independence principle" is one ion's binding to a channel (or translocator in general) particularly strongly (Hille, 1975*b*; McLaughlin, 1977). In this instance, tight binding by Cs^+ inside the pore (see below) could explain most of the differences in the two observed sequences. Deviations from independence have also been attributed to other effects such as "single file diffusion" (e.g., Hodgkin and Keynes, 1955).

We have shown that the selectivity fingerprint of state O_1 (as measured by relative permeabilities or by conductance in symmetrical solutions) is experimentally indistinguishable from that of O_2. In addition, the shapes of the conductance–activity curves and anomalous mole fraction curves are very similar for O_1 and O_2. These observations suggest that the conduction pathway changes very little on transition between O_1 and O_2. A similar proposal has been put forth by Gray et al. (1985) who observed similar selectivities and K^+ binding affinities between substate and main state for the SR K channel from rabbit heart. Given the obvious differences between O_1 and O_2, the similarities in selectivity properties (as well as conductance–activity and anomolous mole fraction behavior) are quite remarkable.

Cs effects

Two measures of the SR K channel's selectivity with respect to Cs^+ gave apparently contradictory results. First, the relative permeability of Cs^+ relative to K^+ was a function of concentration, but varied generally about unity. However, single channel conductance in the presence of Cs^+ alone was 26 pS (O_2) and 15 pS (O_1) (symmetrical 200 mM Cs^+). These values contrast with those observed in the presence of symmetrical 200 mM K^+, e.g., 189 pS for O_2 and 105 pS for O_1. Thus, Cs^+ ions are more permeant than K^+ in the SR K channel but less conductive. In addition, the presence of Cs^+ ions inhibits K^+ permeation through the channel, inducing a rapid type of "blockade" (Fig. 7 *A*) (Cukierman et al., 1985).

Cursory examination of these data suggests that they conflict. However, a consideration of the underlying rate processes shows that permeability and conductance, as measures of selectivity, do not in general agree (Hille, 1975*a*). Selectivity as measured by conductance is expected to be directly comparable to that inferred from permeability ratios only in the limit of negligible occupancy, where conductance is proportional to concentration (i.e., where independence holds).

In biionic conditions, Cs^+ may be considered more permeant than K^+ ions because in the presence of *cis* Cs^+, the reversal potential is more negative than with *cis* solutions of K^+ at the same concentration. However, when Cs^+ and K^+ ions are mixed together, single channel conductance becomes smaller than with either of the pure salt solutions; conductance reaches a minimum at a mole fraction Cs^+ of 0.75 for both O_1 and O_2 (Fig. 9). This finding suggests that Cs^+ is now less permeant than K^+. Such "anomalous mole-fraction" behavior absolutely requires a model in which one permeant ion influences either the channel or another permeant ion during transport (Hille and Schwarz, 1978).

Finally, we must reconcile the fact that Cs^+ is as permeant as K^+ (and under certain conditions more permeant) in the cardiac SR K channel (Figs. 2 and 5) and yet it blocks K^+ current. Clearly the standard notion of a blocking particle that diffuses into the pore, sterically inhibits the movement of ions, and later moves back out of the pore in the same direction from which it entered, is inappropriate. Rather, we postulate that Cs^+ diffuses in and binds to an energetically favorable site for a relatively long time; in doing so it inhibits the transport of K^+ just like a blocker. Later, however, the Cs^+ ion may continue through the pore and thereby contribute an increment of Cs^+ current. It is this additional mechanism of exit from its binding site (continuing through the channel rather than reversing direction and returning from whence it came) that distinguishes the Cs^+ "blocking" reaction.

The phenomenon of low conductance-permeant ion blockade has been reported for a variety of channels. These include Ca^{2+} channels (Hess and Tsien, 1984; Hess et al., 1986; Lansman et al., 1986), sodium channels (Hille, 1975*b*), squid axon K^+ channels (French and Wells, 1977), and the rabbit skeletal muscle SR K channel (Miller et al., 1984; Cukierman et al., 1985).

Modeling conduction

In our analysis of Cs^+ block, we have vacillated between the simple thermodynamic treatment developed by Woodhull (1973) and a nonequilibrium approach based on classical rate theory. Interestingly, both approaches provide useful insight. It is intuitive from an examination of Fig. 7 that the Woodhull-type analysis provides a useful description of the Cs^+ "blocking" reaction under certain conditions. However, this analysis certainly fails to explain the anomalous mole fraction data (not to mention the substantial Cs^+ permeability and its measurable conductance).

As mentioned, we envision the reaction between Cs^+ and the cardiac SR K channel to involve tight binding within the conduction path followed by slow permeation. As more Cs^+ is added to solutions containing K^+, the occupancy of the channel by Cs^+ increases. It follows that total current becomes increasingly dominated by the low conductance Cs^+ ion at the expense of high conductance K^+. Under such circumstances, total current falls so low that simple equations that assume zero current upon "blockade" are acceptable. At some point, however, Cs^+ ions overwhelm K^+ and total current increases, presumably because repulsion between multiple Cs^+ ions within the pore is significant.

In order to model these situations, we adopted a rate theory approach. Also, as conductance in the SR K channel continues to rise monotonically over the activity range 0.2–0.7 M (Fig. 6), we implemented a model in which more than one ion may occupy the channel at any given time. Good fits were obtained for O_2 and O_1. In addition, we obtained excellent fits to the ohmic current–voltage relations using this model. The profile from which the fits were calculated has lateral barriers of equal height and wells of equal depth. In order to fit the monotonically rising phase of the conductance–activity curves between 0.2 and 0.7 M, an ionic repulsion term (=20) was added. This term requires that the K_D for binding of a K^+ ion is 400-fold greater when the adjacent site is occupied as opposed to vacant. That is, occupancy of one binding site raises the energy of the second site by 6 *RT*. Physically, this corresponds to two unliganded ("naked") ions separated by 0.5 nm in a medium of

dielectric constant 20 (a low field strength ion channel with a linear drop in potential between wells).

The theoretical conductance–activity curve calculated from the model exhibits an essentially linear rise in the limit of low ionic activity (14 pS/mM). Not shown in the illustrations is a conductance peak at 245 pS (K^+ activity = 1.5 M) followed by a linear decline phase (−24 pS/M). Finally, the rate of decline slows as conductance approaches zero in the limit of very high concentration.

In the theoretical calculations of channel occupancy (Fig. 10 *B*), the probability of channel vacancy (P_0) falls rapidly in low ionic strength solutions while the probability of single occupancy (P_1) rises rapidly; they cross each other ($P_0 = P_1 = 0.5$) at 5.1 mM K^+. P_1 reaches a maximum and then begins to decline linearly (−0.087 M^{-1}). P_1 crosses the P_2 (probability of double occupancy) curve ($P_1 = P_2 = 0.5$) at 6.7 M K^+ (data not shown). P_2 rises slowly initially but asymptotes to a linear segment whose slope is 0.087 M^{-1} up to 10 M K^+ activity.

Thus, we have seen that calculations based on rate theory using a two-site model adequately account for the current–voltage and conductance versus activity data in K^+. It is almost certain that other profiles exist from which adequate fits can be calculated. To date, we have been unable to model the anomalous mole fraction data or the concentration dependence of $P_K:P_{Cs}$ with a unique two-site profile for Cs^+. However, anomalous mole fraction behavior implies significant interaction among conducting ions.

Multi-ion conduction

Of the several indicators for the multi-ion nature of ionic channels (Hille, 1984), the cardiac SR K channel exhibits three, e.g., a conductance–activity relationship that does not saturate, a non-monotonic relationship between conductance and ionic mole fraction, and a non-monotonic relationship between permeability ratio and ionic activity. Among the indicators that failed are the absence of strong voltage-dependent blockade by Cs^+ and activity-independence of the conductance ratios (K^+ and Na^+). We suggest that our failure to demonstrate activity-dependent conductance ratios may reflect our difficulty in measuring Na^+ conductances below ~100 mM (where ionic conductance diminishes rapidly and the signal-to-noise ratio of the measurements declines substantially). Further, non-saturating conductance–activity behavior can be demonstrated in a single-ion channel if fixed negative charges are concentrated at the pore mouth (Jordan, 1987). Of course, each criterion is consistent with but not necessary for identifying multi-ion occupancy.

Thus, we have demonstrated two strong and one weak argument for the multi-ion nature of the cardiac SR K channel; taken together the three arguments are compelling and lead us to conclude that the channel is indeed multi-ion. Further, the facility with which the two-site model explains the experimental data is consistent with the multi-ion nature of the SR K channel. It strongly suggests that ion–ion interaction occurs, leading to deviation from the independence principle and anomalous mole-fraction behavior.

We are grateful to Drs. P. Labarca, A. O. Grant, S. Simon, and J. W. Moore for fruitful discussions and helpful advice. We thank Dr. G. S. Oxford for providing the initial FORTRAN computer model. We also appreciate the expert technical and secretarial assistance provided by B. Hill and S. Webb.

This work was supported by NHLBI grants HL-19216 and 17670, and NIGMS 5T32 GM-07171 and 07105. R. Coronado was supported by an Established Investigatorship from the American Heart Association.

Received for publication 17 November 1987 and in final form 19 August 1988.

REFERENCES

Bader, H., and A. K. Sen. 1966. (K^+)-dependent acyl phosphatase as part of the (Na^+ + K^+)-dependent ATPase of cell membranes. *Biochim. Biophys. Acta.* 118:116–123.

Begenisich, T., and M. D. Cahalan. 1980. Sodium channel permeation in squid axons. I. Reversal potential experiments. *J. Physiol. (Lond.).* 307:217–242.

Caillé, J., M. Ildefonse, and O. Rougier. 1985. Excitation-contraction coupling in skeletal muscle. *Prog. Biophys. Mol. Biol.* 46:185–239.

Coronado, R., and C. Miller. 1979. Voltage-dependent caesium blockade of a cation channel from fragmented sarcoplasmic reticulum. *Nature (Lond.).* 280:807–810.

Coronado, R., and C. Miller. 1980. Decamethonium and hexamethonium block K^+ channels of sarcoplasmic reticulum. *Nature (Lond.).* 288:495–497.

Coronado, R., and C. Miller. 1982. Conduction and block by organic cations in a K^+-selective channel from sarcoplasmic reticulum incorporated into planar phospholipid bilayers. *J. Gen. Physiol.* 79:529–547.

Coronado, R., R. L. Rosenberg, and C. Miller. 1980. Ionic selectivity, saturation, and block in a K^+-selective channel from sarcoplasmic reticulum. *J. Gen. Physiol.* 76:425–446.

Cukierman, S., G. Yellen, and C. Miller. 1985. The K^+ channel of sarcoplasmic reticulum. *Biophys. J.* 48:477–484.

Eisenman, G. 1961. On the elementary atomic origin of equilibrium ionic specificity. *In* Symposium on Membrane Transport and Metabolism. A. Kleinzeller and A. Kotyk, eds. Academic Press, Inc., New York. 163–179.

Eisenman, G., S. M. Ciani, and G. Szabo. 1968. Some theoretically expected and experimentally observed properties of lipid bilayer membranes containing neutral molecular carriers of ions. *Fed. Proc.* 27:1289–1304.

French, R. J., and J. B. Wells. 1977. Sodium ions as blocking agents and charge carriers in the potassium channel of the squid giant axon. *J. Gen. Physiol.* 70:707–724.

Gordon, L. G. M. 1974. Ion transport via alamethicin channels. *In* Drugs and Transport Processes. B. A. Callingham, ed. University Park Press, London. 251–276.

Gray, M. A., R. A. P. Montgomery, and A. J. Williams. 1985. Asymmetric block of a monovalent cation-selective channel of rabbit cardiac sarcoplasmic reticulum by succinyl choline. *J. Membr. Biol.* 88:85–95.

Hess, P., and R. W. Tsien. 1984. Mechanism of ion permeation through calcium channels. *Nature (Lond.).* 309:453–456.

Hess, P., J. B. Lansman, and R. W. Tsien. 1986. Calcium channel selectivity for divalent and monovalent cations. Voltage and concentration dependence of single channel current in ventricular heart cells. *J. Gen. Physiol.* 88:293–319.

Hille, B. 1975*a*. Ionic selectivity of Na and K channels. *In* Membranes, A Series of Advances. C. Eisenman, ed. Marcel Dekker, Inc., New York. 255–323.

Hille, B. 1975*b*. Ionic selectivity, saturation, and block in sodium channels. A four-barrier model. *J. Gen. Physiol.* 66:535–560.

Hille, B. 1984. Ionic Channels of Excitable Membranes. Sinauer, Sunderland, MA.

Hille, B., and W. Schwarz. 1978. Potassium channels as multi-ion single-file pores. *J. Gen. Physiol.* 72:409–442.

Hodgkin, A. L., and R. D. Keynes. 1955. The potassium permeability of a giant nerve fibre. *J. Physiol. (Lond.).* 128:61–88.

Hungerford, R. T., G. E. Lindenmayer, W. P. Schilling, and E. Van Alstyne. 1984. Effects of membrane potential on sodium-dependent calcium transport in cardiac sarcolemma vesicles. *In* Electrogenic Transport: Fundamental Principles and Physiological Implications. M. P. Blaustein and M. Lieberman, eds. Raven Press, New York. 239–251.

Jones, L. R. 1988. Rapid preparation of canine cardiac sarcolemmal vesicles by sucrose flotation. *Methods Enzymol.* 157:85–91.

Jones, L. R., and H. R. Besch. 1984. Isolation of canine cardiac sarcolemmal vesicles. *In* Methods in Pharmacology. A. Schwartz, ed. Plenum Press, New York. 1–12.

Jordan, P. C. 1987. How pore mouth charge distributions alter the permeability of transmembrane ionic channels. *Biophys. J.* 51:297–311.

Krasne, S. 1980. Ion selectivity in membrane permeation. *In* Membrane Physiology. T. E. Andreoli, J. F. Hoffman, and D. D. Fanestil, eds. Plenum Press, New York. 217–241.

Krasne, S., and G. Eisenman. 1976. The influence of molecular variations of ionophore and lipid on the selective ion permeability of membranes: I. Tetranactin and the methylation of nonactin-type carriers. *J. Membr. Biol.* 30:1–44.

Labarca, P., and C. Miller. 1981. A K^+-selective, three-state channel from fragmented sarcoplasmic reticulum of frog leg muscle. *J. Membr. Biol.* 61:31–38.

Lansman, J. B., P. Hess, and R. W. Tsien. 1986. Blockade of current through single calcium channels by Cd^{2+}, Mg^{2+}, and Ca^{2+}. Voltage and concentration dependence of calcium entry into the pore. *J. Gen. Physiol.* 88:321–347.

Läuger, P. 1973. Ion transport through pores: a rate-theory analysis. *Biochim. Biophys. Acta.* 311:423–441.

McKinley, D., and G. Meissner. 1978. Evidence for a K^+, Na^+ permeable channel in sarcoplasmic reticulum. *J. Membr. Biol.* 44:159–186.

McLaughlin, S. 1977. Electrostatic potentials at membrane-solution interfaces. *Curr. Top. Membr. Transp.* 9:71–144.

Meissner, G., and D. McKinley. 1982. Permeability of canine cardiac sarcoplasmic reticulum vesicle to K^+, Na^+, H^+ and Cl^-. *J. Biol. Chem.* 257:7704–7711.

Miller, C. 1978. Voltage-gated cation conductance channel from fragmented sarcoplasmic reticulum. Steady state electrical properties. *J. Membr. Biol.* 40:1–23.

Miller, C., and E. Racker. 1976. Ca^{++}-induced fusion of fragmented sarcoplasmic reticulum with artificial planar bilayers. *J. Membr. Biol.* 30:283–300.

Miller, C., J. E. Bell, and A. M. Garcia. 1984. The potassium channel of sarcoplasmic reticulum. *Curr. Top. Membr. Transp.* 21:99–132.

Mueller, P., D. O. Rudin, H. T. Tien, and W. C. Wescott. 1962. Reconstitution of excitable cell membrane structure in vitro. *Circulation.* 26:1167–1171.

Myers, V. B., and D. A. Haydon. 1972. Ion transfer across lipid membranes in the presence of gramicidin A. II. The ion selectivity. *Biochim. Biophys. Acta.* 274:313–322.

Skou, J. C. 1960. Further investigations on a Mg ion- and Na ion-activated adenosine triphosphatase, possibly related to the active, linked transport of Na ion and K ion across the nerve membrane. *Biochim. Biophys. Acta.* 42:6–23.

Tomlins, B., and A. J. Williams. 1986. Solubilisation and reconstitution of the rabbit skeletal muscle sarcoplasmic reticulum K^+ channel into liposomes suitable for patch clamp studies. *Pfluegers Arch. Eur. J. Physiol.* 407:341–347.

Tomlins, B., A. J. Williams, and R. A. P. Montgomery. 1984. The characterization of a monovalent cation-selective channel of mammalian cardiac muscle sarcoplasmic reticulum. *J. Membr. Biol.* 80:191–199.

Woodhull, A. M. 1973. Ionic blockade of sodium channels in nerve. *J. Gen. Physiol.* 61:687–708.